

# Widely Tunable Narrow-Linewidth Monolithically Integrated External-Cavity Semiconductor Lasers

Tin Komljenovic, Sudharsanan Srinivasan, Erik Norberg, Michael Davenport, Gregory Fish,  
and John E. Bowers, *Fellow, IEEE*

**Abstract**—We theoretically analyze, design, and measure the performance of a semiconductor laser with a monolithically integrated external cavity. A  $\sim 4$  cm long on-chip cavity is made possible by a low-loss silicon waveguide platform. We show tuning in excess of 54 nm in the O-band as well as significant reduction in laser linewidth due to controlled feedback from the external cavity. The measured linewidth in full tuning range is below 100 kHz and the best results are around 50 kHz. Approaches to further improve the performance of such laser architectures are described.

**Index Terms**—Semiconductor lasers, cavity resonators, laser tuning, photonic integrated circuits.

## I. INTRODUCTION

PHOTONIC integration brings a promise of significant cost, power and space savings in today's optical data transmission networks and sensor applications. Monolithic integration using heterogeneous processes assembles many devices or optical functionalities on a single chip so that all optical connections are on chip and require no external alignment and has the further promise of improved performance, which we demonstrate here.

Monolithic integration has been demonstrated on both indium phosphide (InP) and silicon (Si) substrates. Integration on Si substrates has been a major area of research in recent years [1] with goals of lower cost and higher volume manufacturing. Heterogeneously integrating III-V materials on silicon also improves individual device performance, mainly due to lower losses and better lithography. As optical communications shift to more complex modulation formats, narrow linewidth lasers become a necessity. For example, a 16-QAM modulation format requires a laser linewidth  $< 300$  kHz [2]. Furthermore for DWDM based systems, lasers have to be tunable to align to a certain grid. Tuning can also be exploited in switching scenarios and for improving network resilience to downtime and typically requires tuning across the communication band. Sensors are another area that can benefit from tunable, narrow-linewidth lasers. There have been many results prior to this work addressing this need [3]–[16] and we compare to them in the measurement section.

Manuscript received January 27, 2015; revised March 26, 2015; accepted April 10, 2015. This work was supported by a DARPA EPHI contract. The work of T. Komljenovic was supported by NEWFELPRO Grant No. 25.

T. Komljenovic, S. Srinivasan, M. Davenport, and J. E. Bowers are with the University of California Santa Barbara, Santa Barbara, CA 93106 USA (e-mail: tkomljenovic@ece.ucsb.edu; sudhas@ece.ucsb.edu; davenport000@gmail.com; bowers@ece.ucsb.edu).

E. Norberg and G. Fish are with Aurion Inc., Goleta, CA 93117 USA (e-mail: erik.norberg@aurion.com; greg.fish@aurion.com).

Color versions of one or more of the figures in this paper are available online at <http://ieeexplore.ieee.org>.

Digital Object Identifier 10.1109/JSTQE.2015.2422752

In this paper we theoretically analyze, design, and measure the performance of a semiconductor laser with a monolithically integrated external cavity. Controlling the feedback from the integrated external cavity to the laser is essential to improve the performance, just as with an external cavity laser. The advantages of monolithic integration are improved stability, no anti-reflection coating of the laser facet, no external alignment of mirrors, and lower losses from mode-mismatch. The length of the external cavity is around 4 cm, which is an order of magnitude longer than the laser cavity. By optimizing the feedback from such a cavity, we are able to improve the laser performance and show wide tuning in excess of 54 nm with linewidths below 100 kHz across the full tuning range, and best linewidths of 50 kHz.

The paper is organized as follows. In Section II we briefly outline the theory of laser feedback and link it to specifics of the monolithically integrated external cavity. In Section III we give a theoretical analysis of the influence of the external cavity and its influence on laser linewidth, modulation response and relative intensity noise (RIN). Measured results are presented in Section IV, and finally in Section V, we conclude the paper and give several suggestions on further improving the performance of lasers with a monolithically integrated external cavity.

## II. EXTERNAL CAVITY LASERS

### A. Overview

Semiconductor laser behavior, as is very well known, can be significantly affected by external optical feedback. In most situations, one wants to suppress the feedback as much as possible, but controlled feedback can improve certain laser parameters and has therefore been extensively studied.

The study of the effects of optical feedback on semiconductor lasers is made more difficult by at least three things [17]: (i) the broad gain spectrum which permits higher-order longitudinal mode interaction with small changes in feedback conditions, (ii) strong dependence of crystal refractive index on temperature, and (iii) strong dependence of the gain medium refractive index on the excited carrier density. Furthermore, the effects of optical feedback are expected to differ depending on the distance between the laser diode and the external reflector. For distances smaller than the coherence length, the laser and the external reflector behave as a compound cavity. Depending on specific conditions, optical feedback has been shown to make the laser multi-stable, have hysteresis phenomena, enhance, prolong or suppress the relaxation oscillation in the transient output, improve the laser's performance through noise suppression,

reduced nonlinear distortion and modulation bandwidth enhancement and, what is most relevant to our study, improve the laser linewidth [18]–[23].

The effects of feedback are typically divided into five distinct regimes with well-defined transitions [24]. The classical paper from 1980 has been revisited recently and expanded [25]. It is shown that the change of amplitude signal ( $\Delta E$ ) always accompanies that of frequency change ( $\Delta \nu$ ) due to feedback. The dependence is sinusoidal for weak feedback ( $\Delta E \approx E_0 \cdot \cos(2kL)$ ,  $2kL$  being the optical phase associated with distance to external reflector) and becomes more complicated leading to switching, hysteresis and chaos for higher levels of feedback. The full dynamics are complex and depend on many laser parameters such as gain, loss, photon and carrier lifetime and, above all, the linewidth enhancement factor  $\alpha_H$ . Nevertheless, we utilize this dependence of laser output power ( $P \approx E^2$ ) on the phase of feedback signal as an easier way of estimating feedback by monitoring the output power via integrated monitor photodiode.

The feedback behavior can further be separated in four distinct regions: *short* versus *long* cavities and *coherent* versus *incoherent* feedback. The latter condition relates the external cavity length  $L$  to the coherence length  $L_{\text{coh}}$  of the unperturbed source. In our case, the feedback is always coherent in all cases, as the external cavity length is  $\sim 4$  cm in silicon (around 15 cm in air). It is interesting to point out that semiconductor lasers are also sensitive to incoherent return signal as it can deplete carriers changing both the gain and the phase inside the cavity.

The distinction between short and long cavities is made based on the relation between the relaxation resonance frequency ( $f_R$ ) and the external cavity frequency [26] (for short cavities the length  $L < c/(2f_R)$ ), and the oscillation regime is dependent upon the phase of the external path length. For long cavities ( $L > c/(2f_R)$ ), no dependence of the oscillation regime on phase should be observed. We return to the distinction of short and long cavities in the results section.

For narrow-linewidth operation one would typically want to operate in the so-called regime V characterized by the high level of relative feedback (higher than  $-10$  dB). Furthermore it is beneficial to make the cavity longer than the relaxation oscillation frequency as this ensures that the laser output is not dependant on the phase of the returned signal. In traditional external-cavity lasers, one has to typically anti-reflection coat the laser diode front-facet to be able to reach the levels of feedback needed for regime V. With monolithic integration the coating step is avoided and the excess losses associated with optical mode mismatch when coupling back to the laser are completely avoided or minimized by proper taper design.

### B. Monolithically Integrated External Cavity Laser

A schematic of the monolithically-integrated widely-tunable laser with external cavity is shown in Fig. 1. The lasers were designed at UCSB and fabricated using a heterogeneous photonic integration process design kit (PDK) and foundries developed under the DARPA EPHI program [27]. The gain section (SOA1) is inside a 2 mm long cavity formed by loop-mirrors. The

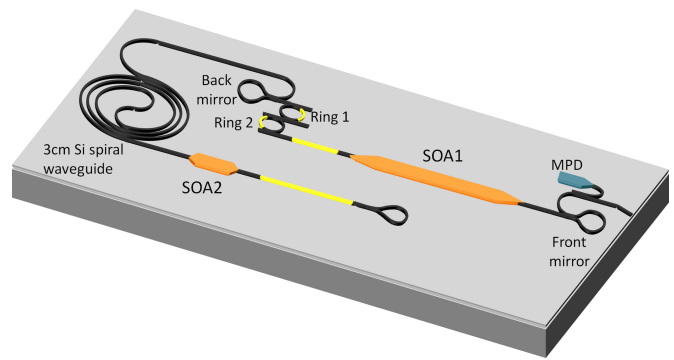


Fig. 1. A schematic view of a tunable laser design with integrated external cavity. Tuners are yellow (two phase sections and two rings for wide tuning), and SOAs are dark orange (SOA1 is the laser active section, and SOA2 is used as an ON/OFF switch or to control the level of feedback). The monitor photodiode (MPD) in blue is used to measure the laser output power for adjustment of laser parameters.

lasing wavelength is determined in the tuning section comprising two ring resonators and a cavity phase section, all of which are controlled by thermal phase tuners. The front loop mirror (at the output of the laser) has a 10% power reflection and the output of the laser is terminated at the facet at an angle of  $7^\circ$  to minimize reflections. The back loop mirror, after the wavelength tuning section, has a power reflection of 60%, which couples part of the light to the external cavity. In order to allow for a long external cavity, a low-loss waveguide platform is needed. Here we utilize optimized silicon waveguides with a loss of 0.67 dB/cm. The external cavity is  $\sim 4$  cm long and has its own phase adjustment section and gain section (SOA2). As the propagation loss in Si waveguides is very low, there is quite strong feedback from the external cavity ( $\sim 5$  dB loss for round-trip). The feedback is present even when the SOA2 is reverse-biased, possibly from reflections at the tapers to the gain region or due to insufficient attenuation of the reverse-biased SOA2. We return to this topic in more detail in the measurement section. The external cavity is coupled on the side with the tuning section so that the tuning rings filter out any spontaneously emitted light from the SOA2 in the extended cavity, improving the phase noise and consequently the linewidth performance. The SOA2 can be forward biased to reduce the losses and amplify the light, or the extended cavity can lase by itself at a sufficiently high bias.

## III. THEORY

We present the necessary equations that govern the linewidth, RIN and modulation response of the fabricated external cavity laser. We include some necessary measurements to verify the theory throughout this section.

### A. Laser Linewidth

The expressions shown in this section are re-derived from [17] and [28]. The laser cavity is modeled as shown in Fig. 2. The tunable single-wavelength filter is designed using the Vernier effect from the drop port response of two ring resonators with

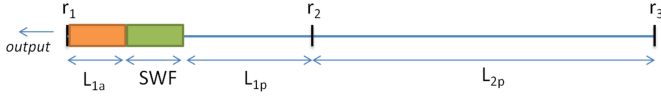


Fig. 2. Schematic of the laser used for modeling. SWF—single wavelength filter. Orange rectangle—gain section.

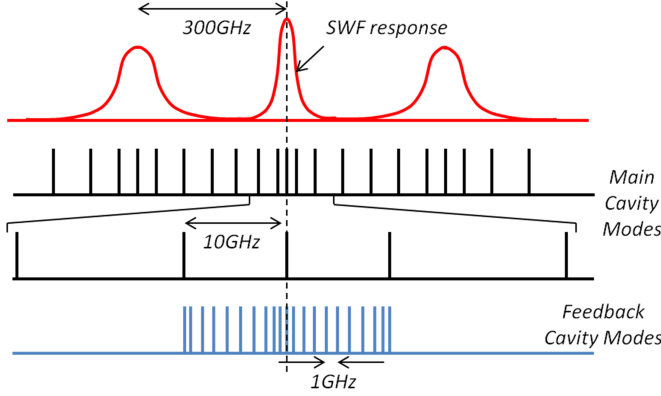


Fig. 3. The mode locations in the main cavity and the feedback cavity, showing non-uniform mode spacing. Only a few modes are shown for simplicity.

slightly different radii. We would like to study modes from two base cavities: One formed between  $r_1$  and  $r_2$  which we call the main cavity, and the other between  $r_2$  and  $r_3$  which we call the feedback cavity. Fig. 3 shows the mode spacing from the two cavities. We observe that the mode spacing is not uniform due to the cavity length enhancement or enhanced photon lifetime for wavelengths near the ring resonator transmission maximum. This is true even for the feedback cavity modes as the photon lifetime is enhanced for the wavelengths around the main cavity modes. We see this effect in the modulation response of the device, as shown later in the text. The feedback cavity length is nearly ten times the main cavity length and hence has much smaller longitudinal mode spacing.

In order to determine the linewidth reduction factor, we find the effective reflectivity of the cavity to the right of the gain section. This can be done in two steps. First, we consider the single wavelength filter (SWF) and the passive section ( $L_{1p}$ ) along with  $r_2$  to form an effective wavelength dependent high  $Q$  mirror with reflectivity  $r_{\text{eff}}$ . Second, we derive the net reflectivity ( $r'_{\text{eff}}$ ) including the external cavity as a response from a Fabry–Perot filter with reflectivities  $r_{\text{eff}}$  and  $r_3$ . The expression for  $r_{\text{eff}}$  and  $r'_{\text{eff}}$  are

$$r_{\text{eff}} = r_2 X^2 \left( \frac{|\kappa|^2 Y}{1 - \tau^2 Y^2} \right)^2 \left( \frac{|\kappa|^2 Z}{1 - \tau^2 Z^2} \right)^2 \quad (1)$$

$$X = e^{-\alpha_p L_{1p}} e^{-j\beta_p L_{1p}} \quad (2)$$

$$Y = e^{-\alpha_p \pi R_1} e^{-j\beta_p \pi R_1} \quad (3)$$

$$Z = e^{-\alpha_p \pi R_2} e^{-j\beta_p \pi R_2} \quad (4)$$

$$r'_{\text{eff}} = \frac{r_{\text{eff}} + r_3 W}{1 + r_{\text{eff}} r_3 W} \quad (5)$$

$$W = e^{-2\alpha_p L_{2p}} e^{-2j\beta_p L_{2p}} \quad (6)$$

where  $R_1$  and  $R_2$  are the radii of the ring resonators.  $\alpha_p, \beta_p$  are the waveguide electric field propagation loss and the effective propagation constant for the lasing mode respectively.  $\kappa$  and  $\tau$  are the coupling and transmission field coefficients respectively for the couplers used in the rings. The linewidth reduction  $F^2$  is then given by the following expressions [28]

$$A = \frac{1}{\tau_{\text{in}}} \text{Re} \left\{ i \frac{d}{d\omega} \ln r_{\text{eff}}(\omega) \right\} \quad (7)$$

$$B = \frac{\alpha_H}{\tau_{\text{in}}} \text{Im} \left\{ i \frac{d}{d\omega} \ln r_{\text{eff}}(\omega) \right\} \quad (8)$$

$$F = 1 + A + B \quad (9)$$

$$\Delta\nu = \frac{\Delta\nu_0}{F^2} \quad (10)$$

where  $\alpha_H$  is the linewidth enhancement factor.  $\tau_{\text{in}} = 2n_{\text{eff}}L_{1a}/c$  where  $n_{\text{eff}}$  is the effective index of the gain section and  $c$  is the speed of light respectively.  $\Delta\nu$  and  $\Delta\nu_0$  are the linewidths with and without the high  $Q$  cavity enhancement respectively. The  $A$  term, corresponding to the linewidth reduction from reduced longitudinal mode confinement, is often denoted as the ratio of the external cavity path length to the gain section path length. The  $B$  term corresponds to the reduction from the negative feedback effect where a decrease in wavelength increases reflectivity (increasing photon density in the main cavity) and hence decreases carrier density, which in turn causes the wavelength to increase due to the carrier plasma effect. The phase condition in the cavity is responsible for a slight detuning of the laser oscillation with respect to the minimum cavity loss condition (resonator resonance). This negative feedback effect occurs only on the long wavelength side of the resonance and is optimum at the wavelength of highest slope in the transmission spectrum. On the short wavelength side of the resonance the effect is reversed and operates in positive feedback, broadening the linewidth.

Fig. 4 shows the effective reflection spectrum (a) and phase (b) for the laser without the feedback cavity. The lasing wavelength is decided by the phase condition  $\varphi_{\text{SOA1}} + \angle r_{\text{eff}}(\omega) = 2\pi$  where  $\varphi_{\text{SOA1}}$  is the roundtrip phase acquired in the gain section. Fig. 4(c) shows the wavelength dependent linewidth reduction. The wavelength dependence is asymmetric with respect to the resonance wavelength and the peak reduction is observed on the red side of the resonance. We observe this asymmetric dependence of linewidth reduction by tuning the phase of the main cavity with a thermal tuner and recording the linewidth. Increasing the tuner current (or power) red shifts the lasing wavelength and decreases the linewidth. Fig. 4(d) shows the measured linewidth as a function of input tuner power. We see a reduction in linewidth from  $\sim 4$  MHz to 375 kHz. We believe this is due to an increase in  $F$  from 3 to 9.6 over  $\pi$  radians. The pattern repeats after a phase change of  $2\pi$  as the laser mode hops to the next cavity mode and the linewidth reduction process repeats.

We can replace  $r_{\text{eff}}$  with  $r'_{\text{eff}}$  in Eqns. (7), (8) to get the linewidth reduction with the external cavity. Fig. 5(a) shows the

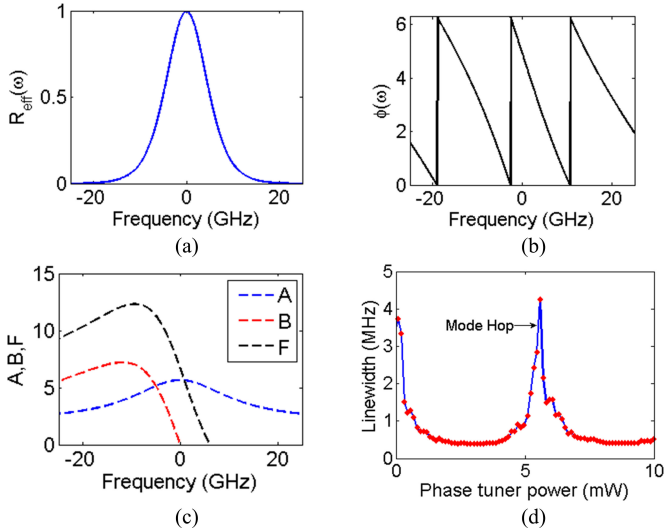


Fig. 4. Normalized reflection (a), phase (b) and linewidth reduction factor (c) of the laser without external cavity as a function of frequency offset from resonance ( $\alpha_H = 4$ ). (d) Measured linewidth (red diamonds) as a function of laser phase tuner power. The blue line is a guide to the eye.

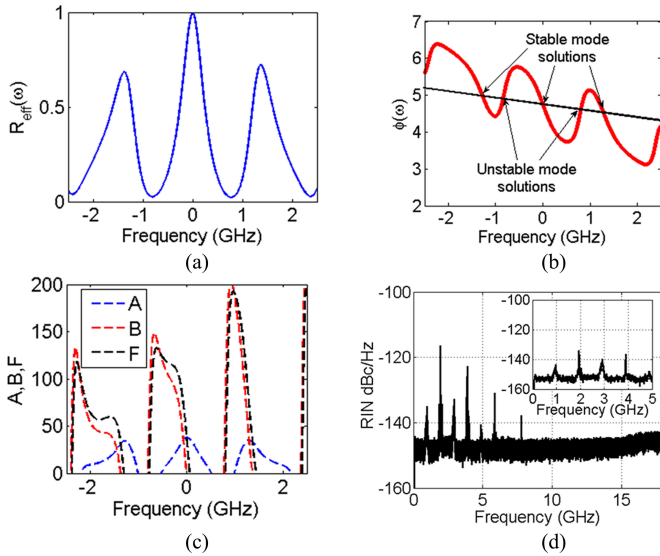


Fig. 5. (a) Normalized reflection, (b) phase and (c) linewidth reduction factor of the laser with external cavity as a function of frequency offset from resonance ( $\alpha_H = 4$ ). (d) RIN measurement when external SOA2 is under high bias current (Resolution bandwidth (RBW) – 3 MHz). Inset: Close-up RIN over a narrow frequency range showing alternating broad and narrow peaks. RBW–500 kHz.

reflection spectrum with the external cavity. The original passband shown in Fig. 4(a) is modulated to give rise to a narrower passband (note the change in scale on the  $x$ -axis). The phase condition is shown in Fig. 5(b) and shows an important feature due to the introduction of the feedback cavity. The laser cavity phase condition is met when the sum of the roundtrip phase in the SOA and the phase of the complex mirror reflectivity is  $2\pi$ . This is graphically shown as the intersection of the black line ( $2\pi - \varphi_{SOA1}$ ) and the red line (mirror phase). However, the points indicated unstable correspond to the saddle point

stationary solutions [29]. Hence there exists alternating stable and unstable mode solutions to the extended laser cavity. We observe this phenomenon in the RIN (amplitude noise) measurement when the external SOA2 is biased with a sufficiently large current. As seen in Fig. 5(d) we observe alternating broad and narrow peaks corresponding to the unstable and stable modes respectively. In the linewidth measurement we only observe the stable modes as the unstable modes are either too weak compared to the measurement noise floor or do not have any phase coherence. Fig. 5(c) shows the linewidth reduction achievable. At the cavity resonance the reduction factor is roughly  $\sim 32$  corresponding to a linewidth reduction of  $\sim 1000$ . We show this improvement in the measurement section. Red tuning the wavelength to get higher reduction was difficult in this case due to laser instability from mode hopping. By using higher  $Q$  ring resonators this mode hopping can be quenched.

### B. Modulation Response

We move on to the modulation response of the laser. The expression for the modulation transfer function  $H(\omega)$  is adopted from [17] with the assumption that the lasing wavelength is not detuned from the cavity mode, for simplicity and we find this expression is sufficient to explain the measurements at operating conditions

$$H(\omega) \cong \frac{\omega_R^2}{\omega_R^2 + (j\omega + \gamma)(j\omega + \kappa(1 - e^{-j\omega\tau_{\text{ext}}}))} \quad (11)$$

$$\omega_R^2 = v_g a N_p \left( \frac{1}{\tau_p} - 2\kappa \right) \quad (12)$$

$$\kappa = \frac{(1 - r_2^2) r_3}{r_2} \frac{c}{2n_{\text{eff}}(L_{1a} + L_{1p} + L_r)} \quad (13)$$

$$\tau_{\text{ext}} = 2n_{\text{eff}} L_{2p} / c \quad (14)$$

where  $\gamma$  is the usual definition for the damping factor.  $v_g$ ,  $a$ , and  $N_p$  are the average group velocity, differential gain and photon density respectively.  $\tau_p$  is the photon lifetime in the main cavity.  $L_r$  is the effective length of the pair of rings.  $\tau_{\text{ext}}$  is the round-trip time in the external cavity. Fig. 6 shows the measured and theoretical curves for the modulation response of the laser with and without the external cavity. The measurements were made using a lightwave component analyzer. As discussed earlier, since the external cavity mode spacing is not uniform, the value of  $\tau_{\text{ext}}$  is frequency dependent. We observe this effect as non-uniform peak spacing in the measurement. The error, however, is marginal.

The peak at 8 GHz is from the photon-photon resonance between the lasing mode and the neighboring mode of the main cavity lying within the ring resonator bandwidth. This phenomenon has successfully been modeled [30] and with careful tailoring of the laser parameters, could even be exploited to increase the 3-dB modulation bandwidth of the laser. The feedback from the external cavity helps suppress this peak or in other words improves the SMSR. The ripple in the measurement without feedback is due to reflections in the external cavity and is detailed in Section IV.

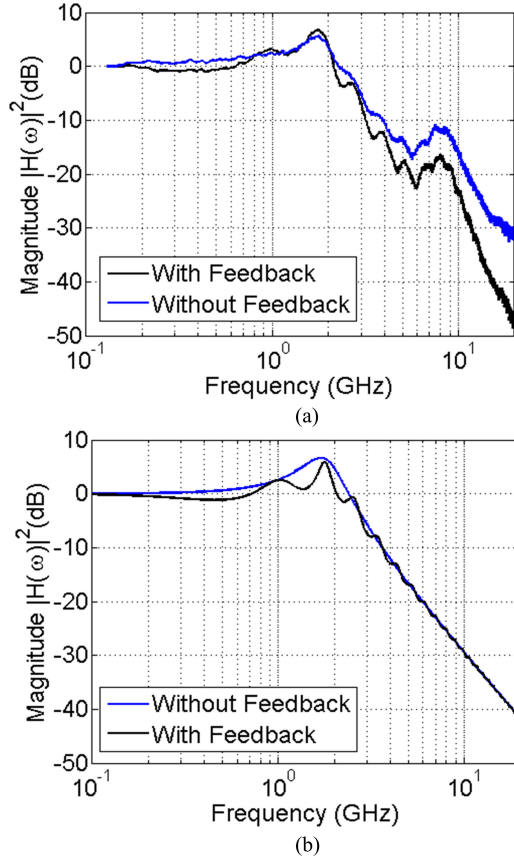


Fig. 6. (a) Measured and (b) theoretical curves for normalized modulation response of the laser with and without external cavity stabilization. The laser quiescent current was 70 mA. The peaks around 8 GHz in measured spectra are due to photon-photon resonance [30] that is not included in our simplified theoretical model.

### C. RIN

The modulation transfer function for small signals shown in Eqn. (11) can be used to model the RIN from the laser [31]. We express RIN per unit bandwidth with the following equation:

$$\frac{\text{RIN}}{\Delta f} = \frac{2h\nu}{P_0} + 16\pi(\Delta\nu_{\text{ST}}) \frac{\omega^2 + (1/\tau_{\Delta N}^2)}{\omega_R^4} |H(\omega)|^2 \quad (15)$$

where  $P_0$ ,  $\Delta\nu_{\text{ST}}$  and  $\tau_{\Delta N}$  are the laser output power from the front mirror, Schawlow-Townes linewidth and the differential carrier lifetime respectively. A comment on detuning the wavelength from the ring resonance frequency to reduce linewidth through the  $B$  term in Eqn. (8) was made earlier. Although beneficial in bringing the linewidth down, biasing on the slope couples frequency noise into amplitude noise [32] and this contribution is not included in Eqn. (15). However, we find this term is negligible for most frequencies. Fig. 7 shows the RIN spectrum, both measurement and theory, for the cases with and without feedback. The measurements were limited by the noise floor of the equipment, and the modulation of the relaxation resonance peak in the case with feedback is barely

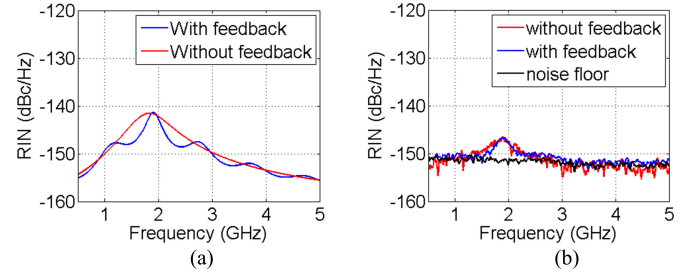


Fig. 7. (a) Theoretical and (b) Measured RIN spectrum with and without external cavity stabilization. RBW=1 MHz.

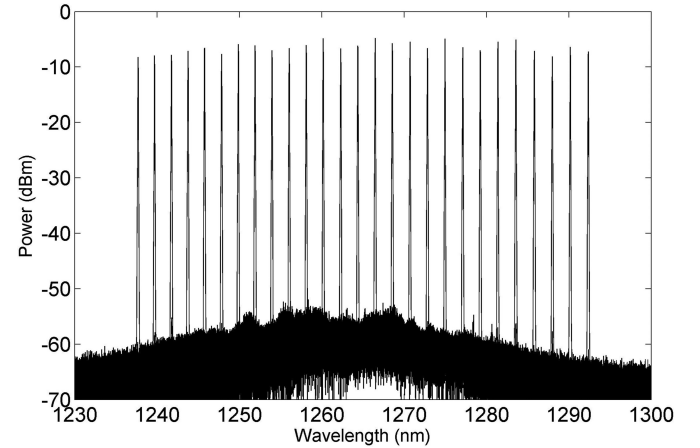


Fig. 8. Lasers are tunable over 54+ nm range with SMSR >45 dB (RBW=0.02 nm).

visible, however, we do observe a narrowing effect of the peak at 1.8 GHz. The RIN is below the noise floor ( $< -150$  dBc/Hz) at all other frequencies not shown in Fig. 7 from 10 MHz to 18 GHz.

## IV. DETAILED MEASUREMENTS

### A. Tunable Laser Performance

The lasers operate in the O-band and are tunable over a 54 nm range from 1237.7 to 1292.4 nm with a high side-mode suppression ratio exceeding 45 dB across the entire tuning range (see Fig. 8). The wide tunability is achieved using the Vernier effect of two rings with different ring radii. The Vernier filter was designed to have a repeat mode spacing of 70 nm. They deliver 10+ mW of output power. The power is somewhat reduced by lower reflection (60%) from the back mirror but could easily be further increased with a booster SOA. The threshold current is in the 30 mA range.

The modulation response and RIN of the laser show three distinct operation regimes: (i) external cavity turned off, (ii) external cavity turned on while keeping the laser single-mode and (iii) external cavity turned on when the laser is operating in several of the external-cavity modes. As there was slight feedback from the external cavity even in the off-state, the modulation

response (see Fig. 6(a)) has a weak super-modulation in all cases.

### B. External Cavity Characterization

The external cavity is coupled through the 60% mirror to the main laser cavity. It is  $\sim 4$  cm long and consists of a 3 cm long spiral (0.67 dB/cm loss), SOA2, phase tuning section and a loop mirror at the end. The idea behind introducing SOA2 into the external cavity is to be able to control the level of feedback to the laser and turn the external cavity completely off. Another option is to introduce a variable optical attenuator (VOA) in the external cavity. We discuss the pros and cons of using either option in Section V.

A severe problem with semiconductor lasers is the extreme sensitivity to feedback and it has been shown to be influenced by feedback levels as low as  $-90$  dB [33]. Such a low level of feedback is unavoidable with monolithic integration. We estimate the reflection from tapers between the silicon waveguides and the III/V gain section in the extended cavity to be in the range of  $-40$  dB resulting with a feedback of around  $-50$  dB when including the propagation loss and the laser back-mirror coupling. The same level of feedback could also come from the external cavity loop mirror if one assumes  $\sim 100\%$  reflectivity and a single-pass absorption of  $\sim 20$  dB from the external SOA2 biased at  $-3$  V. As the free-space length of the cavity is around 15 cm, this automatically places our laser into regime II according to original diagram of Tkach and Chraplyvy [24]. We have not experienced the frequency splitting and mode hopping associated with regime II when measuring the laser with reverse bias applied to the external SOA2. One thing to note is that the relaxation oscillation frequency of the unperturbed laser is around 2 GHz at 70 mA bias, making our external cavity fall in the “long” category [25] and therefore laser oscillation characteristics should not be dependent on the phase of the external path length.

The feedback is definitely present and can clearly be seen when one tunes the external cavity phase heater (positioned after the SOA2 switch) and records the MPD current at the output. We show, in Fig. 9, three sets of such sweeps, one when the SOA2 is reverse biased ( $-3$  V) and two for positive bias of 2.5 and 10 mA. The transparency current for the external SOA2 is around 12 to 15 mA depending on wavelength. The near-sinusoidal modulation of the output power due to phase change of the returned external cavity signal can easily be seen even in case of  $-3$  V of reverse bias of the SOA2. This suggests that the reflection from external cavity back mirror is always present, and is of high enough intensity to influence the laser. This near-sinusoidal modulation becomes further distorted with increased feedback as predicted by [25]. The current at the external phase heater is tuned from 0 to 20 mA delivering up to 200 mW of power to the heater. The efficiency of the external cavity phase tuner is estimated at around 20 mW per  $\pi$  shift. The jump in Fig. 9 comes from laser hopping to a different longitudinal mode. The mode-hopping jump has an expected hysteresis. The behavior is somewhat different if the external

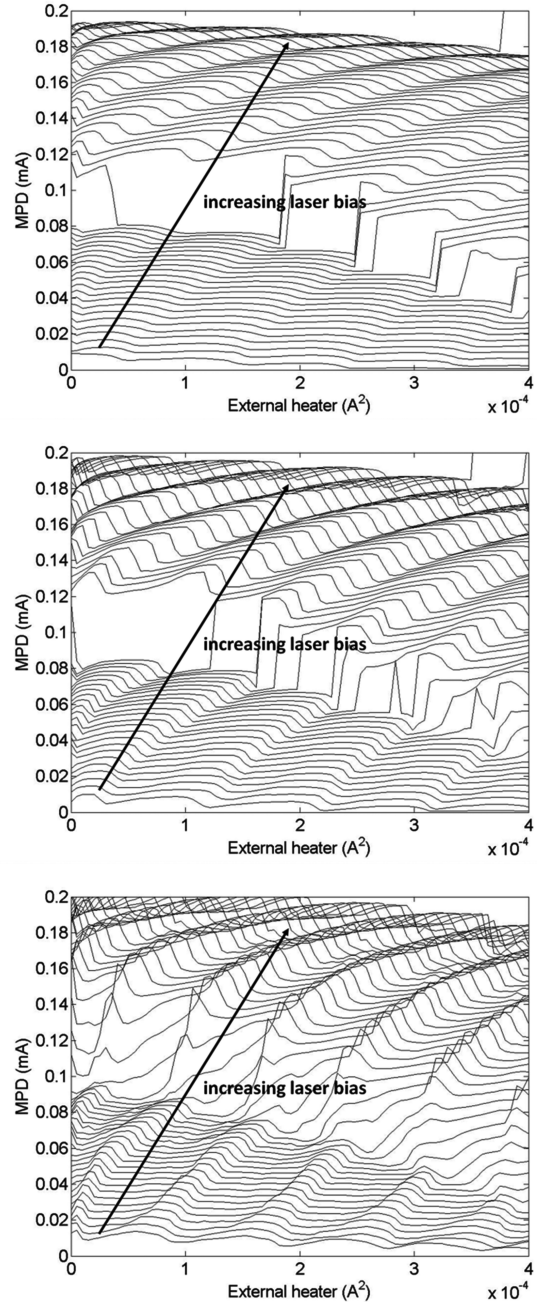


Fig. 9. The influence on laser for three levels of feedback from external cavity: (top) 3 V reverse bias on external SOA2 (middle) 2.5 mA bias on external SOA2 (bottom) 10 mA bias at external SOA2. The x-axis is the squared current ( $I^2 \sim P$ ) applied to external cavity phase tuner, the y-axis is the current collected by MPD at the laser output and every curve corresponds to different laser bias between 30 and 80 mA in steps of 1 mA.

phase heater current is increased or reduced (not shown). If the external SOA2 is driven even stronger, it results in multimode behavior as the rings with measured  $Q$  in the range of 12 000 cannot filter out a single longitudinal mode of the external cavity in our current design (see Section III).

### C. Linewidth

Our main motivation in making a widely-tunable monolithically-integrated laser with external cavity was linewidth reduction due to controlled feedback from the external cavity. One could, in principle, design a single very-long cavity laser utilizing the benefits of the hybrid-silicon platform. Such an approach would lower the longitudinal confinement factor and would result in lower linewidth, but filtering a single-mode from such a cavity would be very challenging and the threshold current would become high. In an external cavity design, one can make a standard single-mode tunable hybrid-silicon laser with low threshold (30 mA range) and provide feedback from an integrated low-loss external cavity in order to reduce the linewidth.

The linewidth measurements were made by the delayed self-heterodyne method. The measurements were averaged 100 times on an electrical spectrum analyzer. With a stable commercial laser, we have verified that the setup can measure linewidths lower than 30 kHz. To minimize external effects, in all measurements we have used an anti-reflection coated lensed fiber tip and two dual stage isolators, each having measured isolation greater than 50 dB. In all linewidth measurements, unless specified otherwise, we have monitored that the laser is indeed single mode by measuring the spectrum with an optical spectrum analyzer and by measuring the laser beat signal with a 10 GHz photodiode. The spacing of mode splitting due to the external cavity is around 0.97 GHz, which is well within the bandwidth of the photodiode. For  $> \sim 12$  mA bias currents to the external SOA2, the external cavity starts to lase and modes separated by ring FSR ( $\sim 300$  GHz) and external cavity stable mode spacing ( $\sim 2$  GHz) appear at the laser output.

The reflection from the external cavity is always present as shown in Fig. 9 and it was practically impossible to measure the performance of the unperturbed laser. As we were unable to completely turn-off the external cavity, we have tried to estimate the linewidth of the unperturbed laser in two ways. First we measured the linewidth of a similar laser design that has no external cavity. This laser has a higher back mirror reflectivity and has a modified silicon waveguide circuit with the same ring resonator geometries for wavelength tuning, however, its length and gain sections are identical. We estimate that higher back-mirror reflectivity reduces the linewidth, but at the same time the somewhat lower  $Q$  of the tuning section increases the linewidth. Measured linewidths of these test structure lasers were 345, 355 and 370 kHz for three devices tested. The corresponding bias currents were 96, 74 and 65 mA.

We also tried to measure the linewidth of the external-cavity laser at low laser bias currents (45 mA) and with external SOA2 reverse biased at  $-3$  V where the influence of external cavity is lowest (see Fig. 9, top image). Linewidths with the external cavity turned off and at 45 mA laser bias were around 300 kHz.

Finally we measured the linewidth of the laser with optimized feedback from the external cavity. The feedback was manually tuned for best performance. We show these results in Fig. 10. The linewidths were below 100 kHz across the entire tuning range and the best single-mode linewidth is 50 kHz. The quoted 3 dB linewidths are calculated from  $-20$  dB points by

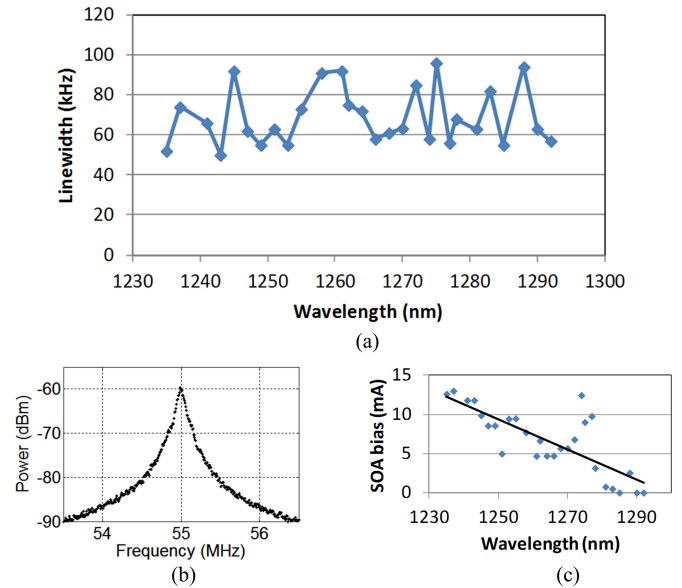


Fig. 10. (a) Measured linewidth across the full tuning range. (b) Measured spectrum for the 50 kHz result (3 MHz span, 30 kHz RBW). (c) Bias currents (blue diamonds) applied to external SOA for linewidths measured and shown in (a) and a trend line (black).

assuming a Lorentzian lineshape [34]. The laser bias currents corresponding to the linewidth results shown are between 75 and 128 mA, while the external SOA2 bias currents are between 0 and 13.06 mA (see Fig. 10(c)). It is interesting to note that the external SOA2 bias currents for minimum linewidth tend to increase as the wavelength decreases. One explanation could be the wavelength dependence of the gain/loss in the external SOA2. Below transparency, the absorption is higher on the blue side of the spectra, so higher bias currents are needed for the same level of feedback. We were able to measure even lower linewidths (below 20 kHz) at higher currents supplied to external SOA2, but the laser was multimode with mode spacing determined by the external cavity length. In this case the RIN and frequency noise spectrums have peaks at this mode separation. This shows that the external cavity can provide even better performance if the filtering section is optimized. We also believe that the external SOA2 increased the noise in the feedback signal due to random spontaneous emission events, thus limiting the linewidth improvement performance over the theoretically predicted one.

The measurements were done on a temperature controlled stage with temperature set at  $20$  °C, but as the lasers were unpackaged and there was no temperature fluctuation feedback applied to the laser, we believe that the performance could be further improved if the lasers were packaged. Nevertheless, to the best of our knowledge, these results set a world record linewidth for a monolithically-integrated widely-tunable laser design (see Fig. 11) [3]–[16]. It should be noted that in [3] (also shown in Fig. 11), the authors demonstrated linewidths in 10 kHz range, but with an assembled hybrid design using butt coupling between InP and Si chips.

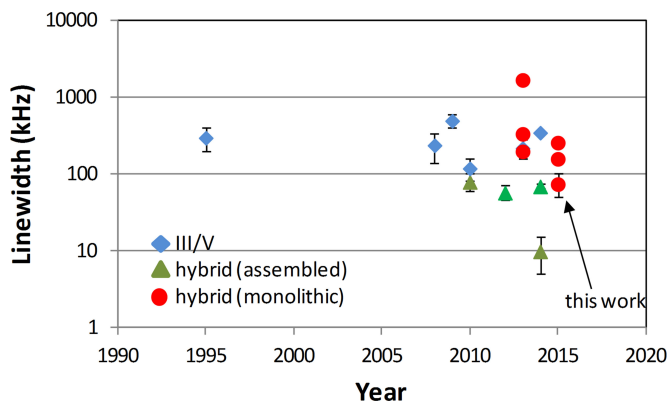


Fig. 11. Widely-tunable integrated lasers linewidth *versus* year. We make distinction between the III/V lasers, and hybrid silicon designs that are assembled or monolithically integrated. This work, to the best of our knowledge, sets a world record linewidth for monolithically-integrated widely-tunable lasers. For references see [3]–[16].

## V. COMMENTS AND CONCLUSIONS

We demonstrated a widely-tunable semiconductor laser with a monolithically integrated 4-cm long external cavity. We have shown tuning in excess of 54 nm around the O-band as well as record linewidths  $< 100$  kHz across the whole tuning range. Such narrow-linewidths allow for more advanced modulation formats in coherent transmission systems leading to better spectral efficiency. The excellent performance is enabled by leveraging the strengths of hybrid integration and low-loss silicon based waveguides. Further performance improvement can be realized by 1) packaging the devices, 2) insulating them from external thermal influences, 3) introducing higher  $Q$  rings in the tuning section and/or 4) increasing the number of rings and consequently increasing the total laser cavity  $Q$ , as well as increasing the length of the external cavity.

In this work we have used an SOA to control the level of feedback, but were unable to completely shut-off the external cavity. The SOA, when driven below transparency, also increases the noise due to random spontaneous emission events potentially limiting the linewidth improvement from the long external cavity. An alternative approach could use a VOA. VOAs could provide a similar functionality with two differences. They only attenuate the signal and so, depending on the configuration, potentially higher levels of feedback (regime V) could not be achieved, and the extinction ratio is typically limited in case broadband operation ( $\sim 60$  nm) is needed. Both the extinction ratio and bandwidth can be improved with cascaded structures but that can complicate the device operation and increase the minimum loss.

The lasers were tuned manually for best performance in terms of narrow linewidth. The procedure for utilizing negative optical feedback could be automated by placing photodiodes in through ports of the tuning ring filters. These photodiodes can be used to map and monitor the precise position of the ring resonance with respect to laser operating frequency.

The demonstrated structures could also be used as chaos or true random bit generators. Compared to previously demon-

strated integrated devices [35], [36], hybrid integrated structures can offer much lower propagation loss in passive section (especially if underlying waveguides are based on ultra-low-loss  $\text{Si}_3\text{N}_4$  platform [37]), thereby allowing for much longer external cavities and/or stronger feedback, potentially easily covering all regimes of feedback outlined in [25].

## REFERENCES

- [1] M. J. R. Heck *et al.*, "Hybrid silicon photonic integrated circuit technology," *IEEE J. Sel. Topics Quantum Electron.*, vol. 19, no. 4, art. no. 6100117, Jul./Aug. 2013.
- [2] M. Seimetz, "Laser linewidth limitations for optical systems with high-order modulation employing feed forward digital carrier phase estimation," in *Proc. Opt. Fiber Commun./Nat. Fiber Opt. Eng. Conf.*, pp. 1–3, Feb. 24–28, 2008.
- [3] N. Kobayashi *et al.*, "Silicon photonic hybrid ring-filter external cavity wavelength tunable lasers," *IEEE J. Lightw. Technol.*, vol. 33, no. 6, pp. 1241–1246, Mar. 2015.
- [4] M. Larson *et al.*, "Narrow linewidth high power thermally tuned sampled-grating distributed Bragg reflector laser," presented at the Opt. Fiber Commun. Conf./Nat. Fiber Opt. Eng. Conf., Anaheim, CA, USA, 2013, Paper OTh31.
- [5] T. Creazzo *et al.*, "Integrated tunable CMOS laser," *Opt. Exp.*, vol. 21, no. 23, pp. 28048–28053, Nov. 2013.
- [6] H. Ishii, K. Kasaya, and H. Oohashi, "Spectral linewidth reduction in widely wavelength tunable DFB laser array," *IEEE J. Sel. Topics Quantum Electron.*, vol. 15, no. 3, pp. 514–520, May/June. 2009.
- [7] G. W. Yoffe *et al.*, "Widely-tunable 30 mW laser source with sub-500 kHz linewidth using DFB array," in *Proc. IEEE 21st Annu. Meeting Lasers Electro-Opt. Soc.*, Nov. 2008, pp. 892–893.
- [8] T. Matsumoto *et al.*, "Narrow spectral linewidth full band tunable laser based on waveguide ring resonators with low power consumption," presented at the Opt. Fiber Commun. Conf., San Diego, CA, USA, 2010, Paper OThQ5.
- [9] H. Ishii *et al.*, "Narrow spectral linewidth full band tunable laser based on waveguide ring resonators with low power consumption," *IEEE J. Sel. Topics Quantum Electron.*, vol. 1, no. 2, pp. 401–407, Jun. 1995.
- [10] H. Ishii, K. Kasaya, and H. Oohashi, "Narrow spectral linewidth operation ( $< 160$  kHz) in widely tunable distributed feedback laser array," *Electron. Lett.*, vol. 46, no. 10, pp. 714–715, May 2010.
- [11] J. Hulme, J. Doyle, and J. Bowers, "Widely tunable Vernier ring laser on hybrid silicon," *Opt. Exp.*, vol. 21, no. 17, pp. 19718–19722, Aug. 2013.
- [12] T. Komljenovic *et al.*, "Narrow linewidth tunable laser using coupled resonator mirrors," presented at the Opt. Fiber Commun. Conf., Los Angeles, CA, USA, 2015, Paper W2A.52.
- [13] S. Keyvaninia, "Demonstration of a heterogeneously integrated III-V/SOI single wavelength tunable laser," *Opt. Exp.*, vol. 21, no. 3, pp. 3784–3792, Feb. 2013.
- [14] K. Nemoto, T. Kita, and H. Yamada, "Narrow-spectral-linewidth wavelength-tunable laser diode with Si wire waveguide ring resonators," *Appl. Phys. Exp.*, vol. 5, art. no. 082701, Aug. 2012.
- [15] T. Kita, K. Nemoto, and H. Yamada, "Long external cavity Si photonic wavelength tunable laser diode," *Jpn. J. Appl. Phys.*, vol. 53, art. no. 04EG04, Feb. 2014.
- [16] Y. Sasahata *et al.*, "Tunable 16 DFB laser array with unequally spaced passive waveguides for backside wavelength monitor," presented at the Opt. Fiber Commun. Conf. Exhib., San Francisco, CA, USA, Paper Th3A.2., Mar. 2014.
- [17] R. Lang and K. Kobayashi, "External optical feedback effects on semiconductor injection laser properties," *IEEE J. Quantum Electron.*, vol. QE-16, no. 3, pp. 347–355, Mar. 1980.
- [18] D. R. Hjelme, A. R. Mickelson, and R. G. Beausoleil, "Semiconductor laser stabilization by external optical feedback," *IEEE J. Quantum Electron.*, vol. 27, no. 3, pp. 352–372, Mar. 1991.
- [19] J. Mark, B. Tromborg, and J. Mark, "Chaos in semiconductor lasers with optical feedback: Theory and experiment," *IEEE J. Quantum Electron.*, vol. 28, no. 1, pp. 93–108, Jan. 1992.
- [20] L. A. Glasser, "A linearized theory for the diode laser in an external cavity," *IEEE J. Quantum Electron.*, vol. QE-16, no. 5, pp. 525–531, May 1980.

- [21] B. Tromborg, J. H. Osmundsen, and H. Olesen, "Stability analysis for a semiconductor laser in an external cavity," *IEEE J. Quantum Electron.*, vol. QE-20, no. 9, pp. 1023–1032, Sep. 1984.
- [22] M. Fleming and A. Mooradian, "Spectral characteristics of external-cavity controlled semiconductor lasers," *IEEE J. Quantum Electron.*, vol. 17, no. 1, pp. 44–59, Jan. 1981.
- [23] L. Goldberg *et al.*, "Spectral characteristics of semiconductor lasers with optical feedback," *IEEE J. Quantum Electron.*, vol. 18, no. 4, pp. 555–564, Apr. 1982.
- [24] R. W. Tkach and A. R. Chraplyvy, "Regimes of feedback effects in 1.5- $\mu\text{m}$  distributed feedback lasers," *IEEE J. Lightw. Technol.*, vol. 4, no. 11, pp. 1655–1661, Nov. 1986.
- [25] S. Donati and R.-H. Horng, "The diagram of feedback regimes revisited," *IEEE J. Sel. Topics Quantum Electron.*, vol. 19, no. 4, art. no. 1500309, Jul./Aug. 2013.
- [26] S. Donati and S.-K. Hwang, "Chaos and high-level dynamics in coupled lasers and their applications," *Progress Quantum Electron.*, vol. 36, no. 2/3, pp. 293–341, Mar.–May 2012.
- [27] A. Fang *et al.*, "Heterogeneous integration on silicon," presented at the Conf. Lasers, Electro-Opt., San Jose, CA, USA, 2014, Paper SM3O.2.
- [28] G. P. Agrawal and C. H. Henry, "Modulation performance of a semiconductor laser coupled to an external high-Q resonator," *IEEE J. Quantum Electron.*, vol. 24, no. 2, pp. 134–142, Feb. 1988.
- [29] J. Mork, B. Tromborg, and J. Mark, "Chaos in semiconductor lasers with optical feedback: Theory and experiment," *IEEE J. Quantum Electron.*, vol. 28, no. 1, pp. 93–108, Jan. 1992.
- [30] A. Laakso and M. Dumitrescu, "Modified rate equation model including the photon–photon resonance," *Opt. Quantum Electron.*, vol. 42, no. 11–13, pp. 785–791, Oct. 2011.
- [31] L. A. Coldren, S. W. Corzine, and M. Masanovic, *Diode Lasers and Photonic Integrated Circuits*. New York, NY, USA: Wiley, 2012.
- [32] K. Aoyama, R. Yoshioka, N. Yokota, W. Kobayashi, and H. Yasaka, "Experimental demonstration of linewidth reduction of laser diode by compact coherent optical negative feedback system," *Appl. Phys. Exp.*, vol. 7, no. 12, pp. 1–3, 2014.
- [33] S. Donati, "Responsivity and noise of self-mixing photodetection schemes," *IEEE J. Quantum Electron.*, vol. 47, no. 11, pp. 1428–1433, Nov. 2011.
- [34] L. B. Mercer, "1/f Frequency noise effects on self-heterodyne linewidth measurements," *IEEE J. Lightw. Technol.*, vol. 9, no. 4, pp. 485–493, Apr. 1991.
- [35] S. Sunada *et al.*, "Chaos laser chips with delayed optical feedback using a passive ring waveguide," *Opt. Exp.*, vol. 19, no. 7, pp. 5713–5724, Mar. 2011.
- [36] A. Argyris, S. Deligiannidis, E. Pikasis, A. Bogris, and D. Syvridis, "Implementation of 140 Gb/s true random bit generator based on a chaotic photonic integrated circuit," *Opt. Exp.*, vol. 18, no. 18, pp. 18763–18768, Aug. 2010.
- [37] J. Bauters *et al.*, "Silicon on ultra-low-loss waveguide photonic integration platform," *Opt. Exp.*, vol. 21, no. 1, pp. 544–555, Jan. 2013.

**Tin Komljenovic** received the M.Sc. and Ph.D. degrees in electrical engineering from the University of Zagreb, Zagreb, Croatia, in 2007 and 2012, respectively. During the Ph.D. degree, he was a Visiting Researcher at IETR, University of Rennes. His current research interests include optical access networks, wavelength-division multiplexed systems and tunable optical sources. He has authored or coauthored more than 30 papers and holds two patents. He is currently working as a Postdoctoral Researcher at the University of California, Santa Barbara, CA, USA, pursuing research in photonic integration. He received the EuMA young Scientist Prize for his work on spherical lens antennas.

**Sudharsanan Srinivasan** received the Bachelor's degree with specialization in engineering physics from the Indian Institute of Technology, Madras, India, July 2009. He is currently working toward the Ph.D. degree at the University of California, Santa Barbara, CA, USA. His research interests include silicon photonics.

**Erik Norberg** received the Ph.D. degree in electrical engineering from the University of California, Santa Barbara, CA, USA, in 2011. At UCSB, he developed integrated photonic microwave filters and a high dynamic range integration platform on InP. He is an author/coauthor of more than 40 papers. He is currently a Senior Optoelectronic Design Engineer at Aurion Inc., Goleta CA, where he is developing integrated Si-photonics components and systems.

**Michael Davenport** received the Undergraduate degree in optical engineering from the University of Alabama, Huntsville, AL, USA, in 2007, and the Master's degree in electrical engineering from the University of California, Santa Barbara, CA, USA, in 2009, where he is currently working toward the Ph.D. degree in electrical engineering. His current research interests include low-noise mode-locked lasers for applications in optical networks microwave photonics, photonic integrated circuits.

**Gregory Fish** received the B.S. degree in electrical engineering from the University of Wisconsin at Madison, Madison, WI, USA, in 1994 and the M.S. and Ph.D. degrees in electrical engineering from the University of California at Santa Barbara, Santa Barbara, CA, USA, in 1999. He is the Chief Technical Officer at Aurion. He is considered a leading expert in the field of photonic integration with nearly 20 years of experience in the field of InP-based photonic integrated circuits. He is an author/coauthor of more than 50 papers in the field and has 12 patents.

**John E. Bowers** (F'93) received the M.S. and Ph.D. degrees from Stanford University, Stanford, CA, USA. He worked for AT& Bell Laboratories and Honeywell before joining the University of California, Santa Barbara (UCSB), CA, USA. He holds the Fred Kavli Chair in Nanotechnology, and is the Director of the Institute for Energy Efficiency and a Professor in the Department of Electrical and Computer Engineering and Materials, UCSB. He is a Cofounder of Aurion, Aerial Photonics and Calient Networks. His research is primarily in optoelectronics and photonic integrated circuits. He received the OSA/IEEE Tyndall Award, the OSA Holonyak Prize, the IEEE LEOS William Streifer Award and the South Coast Business and Technology Entrepreneur of the Year Award. He and coworkers received the EE Times Annual Creativity in Electronics Award for Most Promising Technology for the hybrid silicon laser in 2007. He has published 10 book chapters, 600 journal papers, 900 conference papers, and has received 54 patents. He is a Member of the National Academy of Engineering and a Fellow of the OSA and the American Physical Society.